Published in final edited form as:

Nat Struct Mol Biol. 2015 September ; 22(9): 712–719. doi:10.1038/nsmb.3075.

Ubp6 deubiquitinase controls conformational dynamics and substrate degradation of the 26S proteasome

Charlene Bashore[1], **Corey M. Dambacher**[2], **Ellen A. Goodall**[1], **Mary E. Matyskiela**[1,3], **Gabriel C. Lander**[2], and **Andreas Martin**[1,4]

[1]Department of Molecular and Cell Biology, University of California, Berkeley, Berkeley, CA 94720, USA.

[2]Department of Integrative Structural and Computational Biology, The Scripps Research Institute, La Jolla, CA 92037, USA.

[4]California Institute for Quantitative Biosciences, University of California, Berkeley, Berkeley, CA 94720, USA.

SUMMARY

Substrates are targeted for proteasomal degradation through the attachment of ubiquitin chains that need to be removed by proteasomal deubiquitinases prior to substrate processing. In budding yeast, the deubiquitinase Ubp6 trims ubiquitin chains and affects substrate processing by the proteasome, but the underlying mechanisms and its location within the holoenzyme remained elusive. Here we show that Ubp6 activity strongly responds to interactions with the base ATPase and the conformational state of the proteasome. Electron-microscopy analyses reveal that ubiquitin-bound Ubp6 contacts the N-ring and AAA+ ring of the ATPase hexamer, in close proximity to the deubiquitinase Rpn11. Ubiquitin-bound Ubp6 inhibits substrate deubiquitination by Rpn11, stabilizes the substrate-engaged conformation of the proteasome, and allosterically interferes with the engagement of a subsequent substrate. Ubp6 may thus act as an ubiquitin-dependent timer to coordinate individual processing steps at the proteasome and modulate substrate degradation.

INTRODUCTION

Cell survival fundamentally depends on protein degradation, which in eukaryotes is carried out to a large extent by the ubiquitin-proteasome system (UPS)[1,2]. Cells not only must

Correspondence should be addressed to A.M. (a.martin@berkeley.edu).
[3]Present address: Celgene Corporation, San Diego, CA 92121, USA.

ACCESSION CODES

The electron microscopy density maps for the 26S proteasomes in the presence and absence of ubiquitin-bound Ubp6 can be found at the Electron Microscopy Data Bank under accession numbers 2995 and 6334, respectively.

AUTHOR CONTRIBUTIONS

C.B., E.A.G., M.E.M., and A.M. designed, expressed, and purified proteasome components, and performed biochemical experiments. C.M.D. and G.C.L. performed the electron microcopy, data processing, and segmentation analyses. All authors contributed to experimental design, data analyses, and manuscript preparation.

maintain the proteome and degrade misfolded or damaged polypeptides, but degradation of regulatory and signaling proteins mediates numerous vital processes, ranging from transcription to cell division[3]. As the final destination in the ubiquitin-proteasome system, the essential 26S proteasome is a compartmental protease of the AAA+ family that mechanically unfolds and degrades protein substrates in an ATP-dependent manner. Most proteasomal substrates are marked for degradation and targeted to the proteasome by the enzymatic attachment of ubiquitin chains, which need to be removed by intrinsic deubiquitinases (DUBs) at the proteasome to allow efficient turnover[4,5].

The *S. cervesiae* 26S proteasome consists of at least 34 different subunits that assemble into a 2.5 MDa complex. At the center of the holoenzyme is the barrel-shaped 20S core particle (CP) that sequesters the proteolytic active sites[6]. Access to the degradation chamber is controlled by the 19S regulatory particle (RP), which caps one or both ends of the 20S peptidase and can be further separated into the base and lid subcomplexes. The base contains three non-ATPase subunits, Rpn1, Rpn2 and Rpn13, as well as six distinct AAA+ ATPases (Rpt1-6) that form a heterohexameric ring with a central processing pore, constituting the unfoldase motor of the proteasome. ATP hydrolysis in the AAA+ domains of these ATPases is thought to drive conformational changes and propel movements of conserved pore loops to mechanically pull on substrate polypeptides and translocate them through the central channel into the peptidase[7,89]. In addition to the AAA+ domain, each Rpt subunit contains a N-terminal OB-fold domain that in the hexamer assembles into a distinct N-ring above the AAA+ domain ring. The lid subcomplex acts as a scaffold bound to one side of the base and contains the metalloprotease Rpn11, which is the essential deubiquitinase of the proteasome[4,5]. The base and lid subcomplexes must work together to recognize, process, and ultimately deliver substrates to the proteolytic core particle for cleavage into small peptides. Substrate proteins modified with ubiquitin chains of different linkage types, in particular K11 and K48, but *in vitro* also K63-linked chains[10–12], are tethered to the proteasome by interacting with the intrinsic receptors Rpn10 and Rpn13 or transiently bound shuttle receptors[13–17]. Subsequently, the ATPase ring of the base engages an unstructured initiation region of the substrate and utilizes ATP hydrolysis to mechanically unfold and translocate the polypeptide. Concomitant with substrate translocation is the removal of ubiquitin modifications by the DUB Rpn11, which is localized above the entrance to the central pore of the base[18,19].

Substrate degradation involves multiple conformational states of the proteasome regulatory particle. In the substrate-free state, the AAA+ domains of the Rpts adopt a steep spiral-staircase arrangement that may facilitate substrate engagement[20]. Engagement induces the transition to the actively translocating state that is characterized by a more planar spiral staircase arrangement of the Rpts as well as a coaxial alignment of the N-ring and AAA+ ring with the peptidase, creating a continuous central channel for substrate translocation into the degradation chamber[21,22]. Furthermore, during this conformational change of the regulatory particle, Rpn11 shifts to a central position above the entrance to the pore where it is ideally placed to scan for and remove ubiquitins from substrates as they are translocated by the base ATPases. Thus, we surmise that for every substrate turnover, the proteasome transitions from a substrate-free, engagement-competent state to an engaged state that

facilitates processive translocation, unfolding, and deubiquitination. The proteasome has to switch back to the substrate-free conformation before the engagement of a subsequent substrate.

In addition to Rpn11, the 26S proteasome from *S. cerevisiae* contains another stably associated deubiquitinase, Ubp6, which shows high sequence and structural conservation with its human homologue, Usp14[23]. This 60 kDa ubiquitin specific protease (USP) uses an active site cysteine to cleave the isopeptide bonds within ubiquitin chains. Ubp6 is known to interact with Rpn1 of the base, but efforts to localize either Ubp6 or Usp14 in the context of the proteasome have failed[24,25]. Moreover, Ubp6 has been shown to catalytically and non-catalytically affect the rates of proteasomal degradation. Ubp6 interferes with the critical substrate deubiquitination by Rpn11, stimulates 20S gate opening and thus increases access to the degradation chamber, and enhances the rates of ATP hydrolysis[26–29]. However, the mechanisms by which Ubp6 modulates the activities of the proteasome remain poorly understood.

Depletion of Ubp6 or Usp14 activity has dramatic consequences *in vivo*. Loss of Ubp6 function, for example, increases aneuploidy tolerance in yeast, presumably due to an elevated proteasome capacity for turning over higher protein levels, and pharmacological inhibition of Usp14 in human cells has been shown to stimulate proteasome activity[29–31]. In the hippocampus, loss of Usp14 binding to the proteasome results in higher degradation rates that interfere with presynaptic formation, which can be rescued by overexpression of a catalytically inactive mutant[32]. Thus, both the catalytic and non-catalytic effects of Ubp6 on proteasome activity have important implications in cellular protein turnover. Understanding the interactions of Ubp6 with the proteasome in structural and mechanistic detail is therefore expected to provide important new insights into the role of this deubiquitinase in maintaining the proteome.

In this study we used biochemical and structural approaches on reconstituted proteasome complexes to investigate the nature of Ubp6 interaction. We found that the deubiquitination activity of Ubp6 depends on binding to the base ATPase and responds to the conformational state of the proteasome. By engineering a substrate recruitment system independent of polyubiquitin, we were able to separate catalytic and non-catalytic effects of Ubp6 on proteasomal activities. We localized Ubp6 by electron microscopy and show that it contacts both the N-ring and AAA+ ring of the base in its substrate-engaged conformation, positioning this deubiquitinase directly facing Rpn11. The position of Ubp6 is consistent with our biochemical findings that the ubiquitin-bound deubiquitinase strongly inhibits Rpn11 deubiquitination activity, stabilizes the translocating conformation of the holoenzyme, and prevents engagement of subsequent substrates.

RESULTS

Ubp6 activity responds to proteasome conformational states

The deubiquitination activity of Ubp6 has been shown to dramatically increase upon binding to the 26S proteasome[24,26,29]. To assess the mechanisms of this activation, we measured Ubp6 deubiquitination in the presence of purified proteasome subcomplexes[20] and 4-amino-

methyl-coumarin-fused ubiquitin (Ub-AMC), a substrate that increases fluorescence upon cleavage (Fig. 1). Despite its known interaction with Ubp6, Rpn1 alone failed to stimulate Ubp6 activity, whereas purified base or holoenzyme induced a 300-fold increase in deubiquitination. Thus, full activation of Ubp6 requires contacts with other base subunits in addition to Rpn1 (Fig. 1a).

Interestingly, Ubp6 deubiquitination activity also responds to the conformational state of the proteasome. ATPγS was previously shown to invoke a conformation that is similar to the substrate-engaged state[21,22] (Supplementary Fig. 1). We therefore reconstituted the proteasome in the presence of ATPγS, and observed a 1.9-fold increase in Ubp6 deubiquitination activity compared to the ATP-bound, substrate-free state of the proteasome (Fig. 1a). Importantly, this Ubp6 stimulation was also found for endogenous 26S holoenzyme purified from yeast, suggesting that the deubiquitinase indeed responds to an ATPγS-induced conformational change and not an alternative assembly state during *in-vitro* reconstitution (Fig. 1b). Proteasomes lacking Ubp6 or containing Ubp6 with a mutated active-site cysteine (C118A) did not show this ATPγS-dependent stimulation of deubiquitination, whereas the effect was still observed for proteasomes with the catalytically inactive Rpn11 AXA mutant[4] (Fig. 1b). These results indicate that Ubp6, not Rpn11, is responsible for the stimulated deubiquitination activity in response to the engaged state of the proteasome.

Ubp6 allostery is connected to substrate engagement

Previous studies had shown that polyubiquitin-bound Ubp6 stimulates the ATPase rate of the proteasome[28]. This observation, together with our findings that ATP- and ATPγS-bound proteasomes differentially stimulate the deubiquitination activity of Ubp6, suggest that Ubp6 may play a role in the conformational dynamics of the holoenzyme. The function of Ubp6 in ubiquitin processing during substrate degradation, however, complicates a detailed analysis of such potential allosteric effects. To deliver substrates to the proteasome in an ubiquitin-independent manner, we therefore developed an artificial recruitment system by fusing a permuted single-chain variant of the dimeric substrate adapter $SspB_2$ to the N-terminus of the ATPase subunit Rpt2 (Fig. 2a). In bacteria, $SspB_2$ recruits substrates to the AAA+ protease ClpXP by recognizing a portion of the 11 amino acid ssrA tag[33]. Including this ssrA tag in our model substrates enables their ubiquitin-independent targeting to $SspB_2$-fused reconstituted proteasomes (Fig 2b), which are also still capable of degrading ubiquitinated substrates (Supplementary Fig. 2a). The $SspB_2$-fused proteasomes allowed us to compare how ubiquitin binding to Upb6 and substrate engagement by the AAA+ ring stimulate ATP hydrolysis, and assess whether these processes affect the same or distinct conformations of the proteasome.

To enforce an ubiquitin-bound state of Ubp6, we used the catalytically inactive C118A mutant and incubated it with purified lysine-48 linked ubiquitin dimers[34]. Ubp6 C118A led to a 1.8-fold increase of proteasome ATPase activity only in the presence but not in the absence of di-ubiquitin (Fig. 2c), with comparable effects also observed for ATPase stimulation of the isolated base subcomplex (Supplementary Fig. 2b). The ATPase response of $SspB_2$-fused proteasomes to ubiquitin-bound Ubp6 C118A strongly resembled the

behavior of wild-type proteasomes (Supplementary Fig. 2c), confirming that the $SspB_2$-fusion construct is well suited to separate ubiquitin-related processes from other aspects of substrate degradation. In addition, we covalently modified wild-type Ubp6's active-site cysteine with ubiquitin vinyl-sulfone[35]. The resulting Ubp6-UbVS stimulated the proteasome ATPase activity similar to Ubp6 C118A in the presence of ubiquitin dimers (Fig. 2c), confirming that it is indeed the ubiquitin-bound state of Ubp6 that is responsible for the observed ATPase stimulation.

To analyze the substrate-induced stimulation of ATP hydrolysis, we used the $SspB_2$-fused proteasomes in combination with an ssrA-tagged, permanently unfolded model protein that can get engaged and rapidly translocated without the extra burden of protein unfolding. Processing of this substrate caused a 3.3-fold increase in the ATPase rate of reconstituted proteasomes (Fig. 2c). Importantly, the addition of Ubp6 C118A and di-ubiquitin did not lead to a further increase, suggesting that substrate and ubiquitin-bound Ubp6 stimulate ATP hydrolysis by inducing or stabilizing a similar proteasome state, albeit to a different extent. Our previous structural comparison between substrate-free and substrate-engaged proteasomes suggest that the ATPase stimulation upon substrate engagement is caused by a switching of the AAA+ ring from a steep spiral staircase to a more planar conformation with uniform Rpt-subunit interfaces[21]. Ubiquitin-bound Ubp6 may thus also partially induce or stabilize this engaged conformation of the Rpt ring, which would be consistent with the observed reciprocal stimulation of Ubp6 deubiquitination activity by ATPγS-bound proteasomes.

In support of this hypothesis, we found that substrate engagement and translocation also stimulates Ubp6 deubiquitination activity, albeit not as strongly as trapping the base in a permanently engaged state with ATPγS (Supplementary Fig. 2d). Unfortunately, the ATPγS-bound state prevents substrate engagement and therefore made it impossible to assess whether the ATPase stimulation caused by substrate engagement and ATPγS binding are indeed non-additive, as expected based on the strong similarities between the corresponding proteasome structures[21,22].

In summary, our data suggest that ubiquitin binding to Ubp6 and substrate engagement by the base result in the same proteasome state, marked by an increased ATPase rate and higher Ubp6 deubiquitination activity.

Ubp6 binds to the Rpt hexamer of the base

Previous biochemical studies reported that Ubp6 is tethered to the proteasome through interactions of its N-terminal Ubl domain with the Rpn1 subunit of the base, yet attempts to visualize and localize Ubp6 bound to the proteasome have been unsuccessful[18,19]. The Ubl and the catalytic USP domains of Ubp6 are connected by a flexible 23 amino-acid linker[23], which may allow the deubiquitinase to sample a larger space around the regulatory particle for removal of ubiquitin chains docked on ubiquitin receptors Rpn10 or Rpn13. In addition to this mobile domain architecture of Ubp6, the high intrinsic flexibility of Rpn1, as indicated by consistently lower local resolutions in EM reconstructions[18,19], likely hampered the localization and visualization of proteasome-bound Ubp6.

Given the observed functional crosstalk between ubiquitin-bound Ubp6 and the base ATPase, we concluded that trapping Ubp6 in an ubiquitin-bound state might stabilize it on the proteasome for our EM structural studies. We therefore covalently modified Ubp6's active-site cysteine with ubiquitin vinyl-sulfone[35] and incubated the resulting Ubp6-UbVS with proteasomes in the presence of either ATP or ATPγS. ATP-bound proteasomes with Ubp6-UbVS exhibited a large degree of conformational heterogeneity (Supplementary Fig. 3), which was clearly observed in the 3D classification of the dataset. Although we could distinguish multiple 3D structures representing a continuum of different conformational states of the regulatory particle (Supplementary Fig. 3), none of these reconstructed proteasomes in the presence of ATP contained sufficient particles to accurately localize the Ubp6 density. A 3D refinement of the combined dataset shows the holoenzyme in the apo conformation with diminished density in certain areas of the lid and especially the base, likely indicating the presence of proteasome particles in the engaged or hybrid states (Supplementary Fig. 4). Previous reconstructions of the proteasome with ubiquitin-free Ubp6 did not show such heterogeneity, suggesting that ubiquitin-bound Ubp6 may partially induce alternate conformations. This would be consistent with its stimulation of base ATP hydrolysis. Importantly, we also detected additional weak density next to Rpn1 that contacts the ATPase hexamer and may correspond to a mobile Ubp6-UbVS.

In contrast to the ATP-bound complex, proteasomes incubated with ATPγS and Ubp6-UbVS exhibited less conformational heterogeneity and complete absence of the apo conformation, enabling 3D reconstructions of the holoenzyme in the engaged state (Fig. 3, Supplementary Fig. 5). This reconstruction shows an extra, defined density of appropriate size to accommodate the catalytic domain of Ubp6 or human Usp14 (Fig. 3a). Usp14 and Ubp6 share high structural conservation[23], and we therefore generated a homology model of ubiquitin-bound Ubp6 based on the crystal structure of Usp14-ubiquitin aldehyde (PDB 2AYO[23]), which was then docked into the additional electron density of the ATPγS-bound proteasome complex. Strikingly, the ubiquitin-bound Ubp6 binds directly to the ATPase hexamer of the base, primarily interacting with Rpt1 (Fig. 3a, e). In the docked model, the N-terminus of the ubiquitin-bound catalytic domain is positioned close to the density observed between Ubp6 and Rpn1 (Supplementary Fig. 6), which likely originates from the linker connecting the catalytic domain with the Ubl domain. Ubiquitin-bound Ubp6 contacts both the N-Ring and the AAA+ ring, which in the engaged, translocation-competent state of the base are coaxially aligned with the core particle. Ubp6's position at the periphery of the N-ring places it directly in front of Rpn11, separated by ~30 Å. Especially in its ubiquitin-bound state, Ubp6 may thus sterically occlude Rpn11's access to ubiquitinated substrates, which could explain its previously reported inhibitory effects on Rpn11 DUB activity[26]. Interestingly, this location of the Ubp6 density and its presence in the engaged conformation of the proteasome agree with a previously unspecified density in substrate-processing proteasomes observed by EM tomography of neurons[36].

Ubp6 affects proteasomal conformational dynamics

Given the specific interaction of ubiquitin-bound Ubp6 with the ATPase ring in its engaged, translocation-competent conformation, we wanted to characterize Ubp6's effects on substrate degradation independent of ubiquitin processing. We therefore measured the

ubiquitin-independent, $SspB_2$-mediated degradation of a permanently unfolded model substrate as well as a folded GFP model substrate in the presence or absence of Ubp6 (Fig. 4a). In contrast to the previously reported inhibition of ubiquitin-dependent substrate degradation[26], ubiquitin-free Ubp6 C118A had minimal effect on ubiquitin-independent degradation. However, Ubp6 C118A bound to di-ubiquitin inhibited substrate turnover. This inhibition was observed for degradation of both the folded and unfolded substrates, indicating that ubiquitin-bound Ubp6 does not affect the protein-unfolding abilities of the proteasome. In its ubiquitin-bound state, Ubp6 thus increases the ATPase rate of the base but slows substrate degradation.

One possible explanation for these observations is that Ubp6 stabilizes the engaged, translocation-competent state of the proteasome and inhibits the reversion back to the apo conformation capable of engaging a new substrate. To test this hypothesis we analyzed degradation of the GFP substrate by $SspB_2$-fused proteasomes in the presence of ubiquitin-free or ubiquitin-bound Ubp6 under single-turnover conditions (excess enzyme over substrate), where measured fluorescence signals follow a single-exponential decay (Fig. 4b). Indeed, we observed no effect on single-turnover degradation, consistent with a scenario in which ubiquitin-bound Ubp6 might stabilize, but not strongly induce the substrate-engaged state, allowing efficient engagement of the first substrate. In contrast, multiple-turnover degradation was strongly inhibited by ubiquitin-bound Ubp6 (Fig. 4c). For degradation in the presence of only di-ubiquitin or ubiquitin-free Ubp6, the single-turnover rate constants agree well with the k_{cat} values of multiple turnover. These data thus suggest a model where substrate engagement with the AAA+ ring induces the engaged conformation, which is then stabilized by ubiquitin-bound Ubp6, preventing the return to the apo, engagement-competent conformation until ubiquitin dissociates.

Ubp6 inhibition of ubiquitin-dependent degradation

Most substrates are targeted to the proteasome by attached polyubiquitin chains, which have to be removed by Rpn11 to allow efficient degradation[4,5]. We were thus interested in whether the close proximity of ubiquitin-bound Ubp6 to Rpn11 inhibited Rpn11-mediated deubiquitination and therefore ubiquitin-dependent substrate degradation. We directly analyzed the deubiquitination activity of Rpn11 by measuring Ub-AMC cleavage of holoenzymes with no Ubp6, Ubp6 C118A, ubiquitin-aldehyde (UbH)-modified wild-type Ubp6 or UbH-modified Ubp6 lacking its N-terminal Ubl domain (Fig. 5a). This deubiquitination activity was shown to be highly sensitive to the metal chelator o-phenanthroline, confirming that it originated from Rpn11 (Supplementary Fig 2e). Covalent modification of Ubp6 with UbH ensured an ubiquitin-bound state without adding free di-ubiquitin that would compete in the Rpn11 Ub-AMC cleavage assay. Ubp6-UbH inhibited Rpn11 by 85 %, whereas catalytically inactive Ubp6 C118A showed only 45 % inhibition. Ubp6-ΔUbl did not affect Rpn11 activity, indicating that the functional interaction with Rpn11 and presumably also binding to the Rpt ring itself depend on the Ubl-mediated tethering of Ubp6 to Rpn1.

As a model substrate for the degradation experiments we used a lysine-less variant of superfolder GFP[37] fused to an unstructured region that contained a single lysine for *in vitro*

ubiquitination, thus reducing potential substrate heterogeneity due to multiple chain placements. To ensure a permanently ubiquitin-bound state of Ubp6, we modified its active site with ubiquitin-vinyl sulfone (Ubp6-UbVS). Importantly, Ubp6-UbVS behaves similarly to di-ubiquitin-bound Ubp6 based on the stimulation of proteasomal ATP hydrolysis (Supplementary Fig. 2c). Substrate degradation was measured under single- and multiple-turnover condition using proteasomes purified from an ubp6Δ yeast strain with added-back wild-type Ubp6, Ubp6 C118A, or Ubp6-UbVS (Fig.5 b,c). It is worth noting that in contrast to ubiquitin-independent degradation, all ubiquitin-dependent single-turnover traces followed a double exponential decay, which is consistent with our previously published data[20]. We attribute this behavior to potential heterogeneity in the ubiquitin modification of individual substrate molecules, with shorter ubiquitin chains affecting proteasome binding and processing kinetics. In agreement with earlier reports[26,29], we observed ~ 37 % slower multiple-turnover degradation in the presence of wild-type Ubp6 and a 48 % reduction in rate when the catalytically dead C118A mutant was bound to the proteasome (Fig. 5c). Similar to the results for ubiquitin-independent degradation, there were no substantial defects in single turnover, consistent with our model that, upon ubiquitin binding, Ubp6 may stabilize the engaged proteasome conformation, prevent switching back to the substrate-free conformation, and inhibit engagement of a subsequent substrate for multiple turnover. Proteasomes in complex with Ubp6-UbVS exhibited almost no detectable degradation in both multiple and single turnover (Fig. 5b,c).

Finally, gel-based analyses of the processing of an established poly-ubiquitinated GFP substrate[18,20] revealed that Ubp6-UbVS bound proteasomes do show neither substantial degradation nor deubiquitination (Fig. 5d). This behavior suggests a model in which permanently ubiquitin-bound Ubp6 binds to the ATPase ring right after the substrate has entered the pore and induced the engaged conformation. The position of ubiquitin-bound Ubp6 in proximity to Rpn11 may sterically prevent Rpn11 access to the ubiquitin-modified lysine of our model substrate. Since the proteasome encounters this modified lysine before the GFP moiety, inhibiting ubiquitin-chain removal by Rpn11 would stall translocation and thus prohibit GFP unfolding. However, other substrates may behave differently depending on the substrate geometry and the position of ubiquitin modifications relative to the degradation initiation site. Despite a 45% inhibition of Rpn11 activity by Ubp6 C118A, we did not observe defects in single-turnover substrate degradation for this Ubp6 variant. It is possible that the catalytically inactive Ubp6 C118A is not ubiquitin-bound during degradation of the first substrate, but holds on to ubiquitin after Rpn11 cleavage, affecting Rpn11 deubiquitination and stabilizing the engaged state in multiple turnover. Alternatively, the on- and off-rates for uncleaved ubiquitin on Ubp6 C118A may still allow ubiquitin-chain binding and cleavage by Rpn11, but inhibit the base switching back to the pre-engaged state for multiple turnover. As a control, we verified that the proteasome did not engage and degrade any of the Ubp6 variants, which would also inhibit degradation of our model substrate (Supplementary Fig. 7).

DISCUSSION

Our biochemical and structural data show that, besides its role in ubiquitin cleavage, Ubp6 affects proteasomal substrate degradation by allosterically interfering with distinct

proteasome functions in an ubiquitin-dependent manner. Prior to substrate engagement by the base, Ubp6 is tethered via its Ubl domain to Rpn1, while its catalytic USP domain appears to be rather mobile and sampling a larger area. Interactions of the USP domain with the base ATPase stimulate its deubiquitination activity, likely by changing the conformation of two blocking surface loops, BL1 and BL2[23], and this activity further increases upon proteasome engagement of a substrate polypeptide. Ubiquitin-bound Ubp6 binds and stabilizes this substrate-engaged, translocation-competent conformation of the proteasome by interacting with both the N-ring and the AAA+ ring of the base, thereby maintaining their coaxial alignment with the 20S core. The interaction with the base places ubiquitin-bound Ubp6 in close proximity to Rpn11, where it interferes with Rpn11-mediated substrate deubiquitination. These findings are also consistent with a recent EM-structural study[38].

Our results suggest a model in which substrate engagement acts as a switch to induce the translocation-competent state of the proteasome, which is then regulated by ubiquitin-bound Ubp6 in two ways: the inhibition of Rpn11 and the interference with conformational switching back to the substrate-free state (Fig. 6). Ubp6 would inhibit Rpn11 deubiquitination and therefore slow substrate degradation if it interacts with ubiquitin before Rpn11 has removed all modifications from a translocating substrate. Such coordination between Ubp6 and Rpn11 activities may be important for complex substrates containing multiple, very long, or branched polyubiquitin chains that need to be co-translocationally trimmed by Ubp6. After Rpn11 has cleaved off all ubiquitin modifications and a substrate has been completely unfolded and translocated, Ubp6 may trap the engaged conformation of the proteasome and prevent the engagement of a subsequent substrate until it is no longer occupied with ubiquitin. This mechanism would be important for Ubp6-mediated clearance of polyubiquitin chains from the several ubiquitin receptors before the proteasome commits to the degradation of a new substrate, and it would agree with Ubp6's role in maintaining high levels of free ubiquitin in the cell[39,40].

In our studies we either saturated ubiquitin-binding to catalytically dead Ubp6 or used covalent ubiquitin fusions to exaggerate the effects on proteasomal functions. However, given the fast kinetics of ubiquitin cleavage by Ubp6 compared to Rpn11, wild-type Ubp6 that is processing ubiquitin modifications would not be expected to severely slow proteasomal substrate degradation. Ubp6 may rather act as a timer, not only as previously suggested by trimming of ubiquitin chains and thus affecting the persistence time of substrates at the proteasome, but in an ubiquitin-dependent manner by allosterically coordinating the various substrate-processing steps at the proteasome and preventing stalling of substrates with complex ubiquitin modifications.

Our EM structural work provides the first visualization of ubiquitin-bound Ubp6 in the context of the 26S proteasome. Future higher-resolution structures will be required to elucidate the detailed mechanisms involved in the reciprocal stimulation of Ubp6 deubiquitination and base ATPase activities. It will also be interesting to investigate how Ubp6 coordinates with other proteasome-bound cofactors, for instance the ubiquitin ligase Hul5[24,41,42] or ubiquitin shuttle receptors Rad23, Ddi1, and Dsk2[15,25,43,44], in fine-tuning substrate processing by the 26S proteasome.

METHODS

Yeast strains

Yeast lid and holoenzyme were purified from strain YYS40 (genotype *MAT***a** *ade2-1 his3-11,15 leu2-3,112 trp1-1 ura3-1 can1 Rpn11::Rpn11*-3× Flag(His_3)[48]. Core particle was prepared from either strain RJD1144 (genotype *MAT***a** *his3Δ200 leu2-3,112 lys2-801 trpΔ63 ura3-52 PRE1*-Flag-His_6::*Ylpac211(URA3)*[49] or strain yAM14 (genotype *MAT***a** *ade2-1 his3-11,15 leu2-3,112 trp1-1 ura3-1 can1-100 bar1 PRE1::PRE1*-3× Flag(*KanMX*),[20]). To generate *UBP6* deletion strains, the kanMX6 sequence was integrated at the respective genomic locus, replacing the gene in YYS40[18]. To generate the *UBP6* C118A strain, a C118A copy of Ubp6 was cloned into pRS305 and was integrated into the *UBP6* deletion strain at the *leu2* locus.

Purification of yeast holoenzyme and subcomplexes

Wild-type and mutant proteasome was purified from *S. cerevisiae* essentially as described.[18,21] In summary, holoenzyme, lid, and core particle were purified from yeast strains listed above. Lysed cells were resuspended in lysis buffer containing 60 mM HEPES, pH 7.6, 50 mM NaCl, 50 mM KCl, 5 mM $MgCl_2$, 0.5 mM EDTA, 10% glycerol, and 0.2% NP-40. Holoenzyme lysis also included an ATP-regeneration mix (5 mM ATP, 0.03 mg/ml creatine kinase and 16 mM creatine phosphate). Complexes were bound to anti-Flag M2 affinity resin (Sigma) and washed with wash buffer (60 mM HEPES, pH 7.6, 50 mM NaCl, 50 mM KCl, 5 mM $MgCl_2$, 0.5 mM EDTA, 10% glycerol, 0.1% NP-40 and 500 mM ATP). Core particle was washed with wash buffer containing 500 mM NaCl, and Lid was washed with wash buffer containing 1M NaCl. Complexes were eluted with Flag peptide and separation by size-exclusion chromatography over Superose-6 in gel-filtration (GF) buffer (60 mM HEPES, pH 7.6, 50 mM NaCl, 50 mM KCl, 5 mM $MgCl_2$, 0.5 mM EDTA and 0.5 mM ATP) containing 5% glycerol.

Recombinant expression and purification of proteins and complexes

Base subcomplexes were expressed and purified from *E. col* as previously described.[20] Nine integral subunits (Rpn1, Rpn2, Rpn13, Rpts-1-6,) and four assembly chaperones (Rpn14, Hsm3, Nas2 and Nas6) were expressed with rare tRNAs at overnight at 18 °C after induction with 0.5 mM IPTG. Cells were harvested by centrifugation and resuspended in nickel buffer (60 mM HEPES, pH 7.6, 100 mM NaCl, 100 mM KCl, 10% glycerol, 10 mM $MgCl_2$, 0.5 mM EDTA, and 20 mM imidazole) supplemented with 2 mg ml^{-1} lysozyme, protease inhibitors, (aprotinin, pepstatin, leupeptin and PMSF) and benzonase (Novagen). Cells were lysed with by freeze-thaw cycles and sonication, and clarified by centrifugation. A two-step affinity purification of the base subcomplex was performed using nickel–nitrilotriacetic acid (Ni-NTA) agarose (Qiagen) to select for His_6-Rpt3 and anti-Flag M2 resin (Sigma-Aldrich) selecting for Flag-Rpt1. 0.5 mM ATP was present in all purification buffers. The Ni-NTA and anti-Flag M2 columns were eluted with nickel buffer containing 250 mM imidazole and 0.15 mg ml^{-1} 3× Flag peptide, respectively. The Flag column eluate was concentrated and run on a Superose 6 size exclusion column (GE Healthcare) equilibrated with gel filtration buffer (60 mM HEPES, pH 7.6, 50 mM NaCl, 50 mM KCl, 10% glycerol, 5 mM $MgCl_2$, 0.5 mM EDTA, 1 mM DTT and 0.5 mM ATP).

The GFP fusion substrate construct was cloned into a pET Duet (Novagen) vector, and consisted of a lysinesless superfolder GFP[37], lysineless titin I27 V15P domain, and a random coil containing the ssrA sequence and the PPXY motif. *E. coli* Bl21-star (DE3) cells were transformed with the construct and grown in Terrific Broth (EMD Millipore) at 30 °C. Cells were induced with 0.5 mM IPTG at an OD_{600} of 1–1.5 and expression went for 5 hours at 30 °C.

The unfolded substrate was cloned into a pET 28A (Novagen) vector and consisted of a lysineless, disulfide-less N1 domain from gene-3-protein[50] fused to a random coil containing an ssrA tag, ppxy motif, and a lysineless strepII tag. WT Ubp6 was amplified from genomic (W303) DNA, and cloned into pET Duet with an N-terminal His^6 tag. C118A mutation was made by around-the-horn PCR. *E. coli* Bl21-star (DE3) cells were transformed with either the N1 construct or the Ubp6 constructs and grown in Terrific Broth at 37 °C. Cells were induced with 0.5mM IPTG at an OD_{600} of 0.6 and expression continued overnight at 18 °C.

GFP, unfolded substrate, or Ubp6 expressing cells were harvested by centrifugation and resuspended in nickel buffer (above) supplemented with 2 mg ml^{-1} lysozyme, benzonase (Novagen), and protease inhibitors (aprotinin, pepstatin, leupeptin and PMSF). Cells were lysed by freeze thaw and sonication. Lyates were clarified by centrifugation at 15,000 rpm for 20 minutes at 4 °C. Proteins were purified using Ni-NTA affinity chromatography followed by size exclusion chromatography on a Superdex 200 (GE Healthcare) using nickel and gel filtration buffers mentioned above.

Construction of the $SspB_2$permutant base

To allow ubiquitin-independent substrate delivery to the proteasome, we created a base variant that is fused to a linked permutant dimer of the E.coli substrate adaptor SspB. A wild-type SspB monomer consists of a globular domain and a C-terminal tail of 38 residues. In simple dimer fusions, where we connected the C-terminus of the globular domain of one SspB monomer with the N-terminus of the second SspB monomer, the linker interfered with ssrA substrate binding to $SspB_2$. We therefore constructed a circular permutant SspB monomer, in which we created a new N-terminus at residue L26 and connected the preceding N-terminal helix to the C-terminus of the globular domain, and fused this monomer to the N-terminus of a second, wild-type SspB monomer. The connectivity of this covalently fused dimer is: (L26-D111) - GGASG - (S4-Q25) - GGGTGG - (wild-type monomer). This $SspB_2$ dimer was then fused to the N-terminus of Rpt2 of the base.

Ubiquitin purification and dimer synthesis

Ubiquitin was expressed and purified as previously described[51,52]. Briefly, Rosetta II (DE3) pLysS *Escherichia coli* cells were transformed with a pET28a vector containing the ubiquitin gene from *S. cerevisiae* under control of a T7 promoter. Cells were grown in Terrific Broth supplemented with 1% glycerol at 37 °C until OD_{600} = 1.5–2.0 and were induced with 0.5 mM IPTG overnight at 18 °C. The lysis buffer contained 50 mM Tris-HCl, pH 7.6, 0.02% NP-40, 2 mg mL^{-1} lysozyme, benzonase (Novagen), and protease inhibitors (aprotinin, pepstatin, leupeptin and PMSF). Cells were lysed by sonication and 20 min

incubation at room temperature. Lysate was clarified by centrifugation at 15000 rpm. Clarified lysate was precipitated by adding 60% perchloric acid to a final concentration of 0.5%, and the solution was stirred on ice for a total of 20 min. A 5-mL HiTrap SP FF column (GE Life Sciences) was used for cation-exchange chromatography, and ubiquitin fractions were pooled and exchanged into Ub storage buffer (20 mM Tris-HCl, pH 7.6, and 150 mM NaCl) by repeated dilution and concentration.

Lys-48 ubiquitin dimers were synthesized and purified as previously described[34].

Preparation of Ubiquitin fused Ubp6

50 μM WT Ubp6 or Δubl Ubp6 protein was reacted with 75 μM ubiquitin vinyl sulfone or ubiquitin aldehyde (R&D Systems) in GF buffer at 37 °C. For the experiment in Figure 5d, which required complete inhibition of the active site cysteine, buffer, wild-type Ubp6, or C118A Ubp6 were reacted with ubiquitin aldehyde for seven hours at 37°C in the dark. To ensure complete inactivation, Ubp6-UbH was further reacted with 500 μM NEM for 30 min at 30 °C, followed by quenching with 5 mM DTT for another 30 min at 30 °C. Ubiquitin-aldehyde, NEM, and DTT were removed by dilution and concentration in an Amicon 30K MCWCO concentrator (EMD Milipore).

Ubiquitin AMC hydrolysis assays

Ubiquitin-AMC (R&D systems) hydrolysis was measured in a QuantaMaster spectrofluorimeter (PTI) by monitoring an increase of fluorescence emission at 435 nm with an excitation at 380 nm. Reactions using reconstituted proteasome used 100 nM Ubp6, 150 nM Rpn1, 150 nM recombinant base, 300 nM CP, 300 nM Lid, 300 nM Rpn10, 20 μM unfolded substrate, and 3–10 μM Ub-AMC. Reactions using proteasomes purified from yeast used 100 nM proteasome. Reactions were carried out either in the presence GF buffer (see above) with 1mM DTT and 1× ATP regeneration system or 1 mM ATPgS. Samples were incubated at 30 °C for 5–10 minutes prior to the addition of substrate to ensure Ubp6 association and nucleotide exchange.

ATPase assays

ATPase activity was quantified by an NADH-coupled ATPase assay. Reconstituted proteasomes, (200 nM base, 600 nM core, 600 nM lid, 600nM Rpn10) Ubp6, (200 nM) Ub_2^{K48} (20 μM), and unfolded gene-3-protein substrate (20 μM) were incubated with 1× ATPase mix (3 U ml^{-1} pyruvate kinase, 3 U ml^{-1} lactate dehydrogenase, 1 mM NADH and 7.5 mM phosphoenol pyruvate) at 30 °C. Reactions were done in GF buffer (see above) with 1mM DTT. Absorbance at 340 nm was monitored at 30 °C for 600 s at 1-s intervals by a UV-vis spectrophotometer (Agilent).

Multiple and Single turnover ubiquitin independent degradation assays

26S proteasomes were reconstituted using recombinant, heterologously-expressed $SspB_2$-Rpt2 base, recombinant Rpn10, and lid and core subcomplexes purified from yeast. Multiple turnover degradations were done with 200 nM CP, 600nM Lid, 600 nM base, 600 nM Rpn10, 900 nM Ubp6 and 20 μM Ub_2^{K48}. Reactions were done in the presence of 1× ATP regeneration system (5 mM ATP, 0.03 mg ml^{-1} creatine kinase, 16 mM creatine phosphate)

in gel filtration buffer with 1mM DTT. Single turnover reactions were done with 3 μM $SspB_2$-Rpt2 base, 4.5 μM lid, 4.5 μM base, 4.5 μM Rpn10, 9 μM Ubp6, 20 μM Ub_2^{K48}, and 300 nM substrate in the presence of 1× ATP regeneration system in gel filtration buffer with DTT and ATP regeneration system. GFP single- and multiple-turnover degradation activities were monitored by the loss of GFP fluorescence (excitation, 467 nm; emission, 511 nm) using a QuantaMaster spectrofluorimeter (PTI). Single turnover curves were fit to a single exponential in GraphPad Prism 6.

To track degradation of an unfolded substrate, purified N1 fusion substrates were labeled on a single cysteine with Alexa 647 maleimide at pH 7.2 for 3 hours at room temperature in the dark, before quenching unreacted dye with DTT. Free dye was removed on a Superdex 200. Substrate degradation was measured by taking time-points of a reaction at 30 °C and assessed by SDS-PAGE followed by imaging on a Typhoon Trio (GE) with a 633 nm laser and 670 nm BP emission filter. Band intensity was quantified using Image Quant software. Degradation reactions consisted of 8 μM substrate against proteasomes reconstituted as above with either $SspB_2$-Rpt2 base or WT base to correct for any non-specific, $SspB_2$ independent substrate cleavage.

Preparation of Ubiquitinated substrates

GFP substrates (20 μM) were modified with polyubiquitin chains by 5 μM yeast Uba1, 5 μM yeast Ubc1, 5 μM Rsp5, 1× ATP Regeneration system, and 300 μM ubiquitin. Reaction was carried out in a thermocycler for 2 hours at 25 °C, then overnight at 4 °C.

Multiple and Single turnover ubiquitin dependent degradation assays

GFP constructs were ubiquitinated overnight and then used the next day without freezing. Single- and multiple-turnover degradation activities were monitored by the loss of GFP fluorescence (excitation, 467 nm; emission, 511 nm) using a QuantaMaster spectrofluorimeter (PTI) as above. Multiple turnover reactions consisted of 300 nM purified proteasomes from a ΔUbp6 strain, 600nM Ubp6, and 2μM substrate. Single-turnover reactions consisted of 3 μM proteasome, 6 μM Ubp6, and 300 nM substrate.

For the gel-based assessment of substrate degradation and deubiquitination, 2 μM ubiquitinated EGFP substrate was incubated with 200 nM ΔUbp6 proteasomes in the presence of buffer or 400 nM WT, C118A or UbVS-treated Ubp6. Aliquots at different time points were separated on a SDS-PAGE gel, and the gel was imaged on a Typhoon Trio (GE) with excitation at 488 nM and using a 526 nm SP emission filter.

Electron microscopy

Samples of 26S-bound Ubp6-UbVS were diluted to ~25 nM in 60 mM HEPES pH 7.6, 50 mM NaCl, 50 mM KCl, 5 mM $MgCl_2$, 0.5 mM EDTA, 1 mM TCEP and either 1 mM ATP or 1 mM ATPgS (Sigma). A thin layer of carbon was applied to 400-mesh Cu-Rh maxtaform grids (Electron Microscopy Sciences) by chemical vapor deposition, and grids were subsequently exposed to a 95% Ar/5% O2 plasma for 20 seconds to glow-discharge/ activate the carbon surface. Grids were pre-treated with 4 μl of 0.1% poly-L-lysine hydrobromide (Polysciences) to prevent preferred orientation of 26S particles on carbon.

Poly-L-lysine solution was then wicked away, grids were washed with 4 μl of H_2O, and 4 μl of sample was applied. 252 and 357 images of negatively stained (2% uranyl formate) 26S-Ubp6-UbVS complexes in the presence of ATP or ATPgS, respectively, were collected at a nominal magnification of 52,000 × on an F416 CMOS 4K × 4K camera (TVIPS) with a pixel size of 2.05 Å/pixel at the sample level. Images were acquired on a Tecnai Spirit LaB_6 electron microscope operating at 120keV, with a random defocus range of −0.5 μm to −1.5 μm and an electron dose of 20e-/$Å^2$. Data were acquired using the Leginon automated image acquisition software[53].

Processing

All image preprocessing and 2D analysis was performed using the Appion image-processing pipeline[47]. CTF was estimated using CTFFIND3, and only micrographs having a CTF confidence greater than 80% were used for processing. Particle picking was performed using the template-based FindEM software[54]. Micrographs were phaseflipped using EMAN's "applyctf" function, and particles were extracted with a box size of 384 pixels. Pixel values 4.5 sigma above or below the mean were replaced with the mean intensity of the extracted particle using XMIPP. Multiple rounds of iterative MSA/MRA was used for 2D classification and alignment of the particles, and class averages containing single-capped proteasomes, as well as damaged, aggregated, or false particles, were removed, resulting in a dataset containing 24,411 and 18,565 double-capped proteasome particles in presence of 1mM ATP and 1mM ATPgS, respectively. 3D classification and 3D refinement were performed with C2 symmetry imposed using RELION v1.31[55]. The 3D reoconstructions for proteasomes in the presence of ATP and ATPgS resolved to 24.2 Å and 22.3 Å, respectively, according to a gold standard Fourier Shell Correlation at 0.143. Low resolution intensities were dampened using a SPIDER script in order to more clearly visualize domain features.

3D modeling

An atomic model of yeast Ub-bound Ubp6 was constructed by superimposing the yeast Ubp6 crystal structure (PDB 1VJV) onto the stucture of the human Rsp14 structure bound to Ubiquitin (PDB 2AYO)[23], using UCSF Chimera's "MatchMaker" tool. These structures have high structural homology, and the resulting hybrid structure did not exhibit any clashes between the Ubiquitin and Ubp6. This Ubp6-Ub model was docked into the density putatively corresponding to Ubp6. PDB 4CR4[45] was used for docking other 26S core, base and lid subunits into the ATPγS electron density map obtained here, with the exception of the Rpn8-Rpn11 dimer, for which PDB 4O8Y[46] was used. All docking of PDB structures was performed using the "Fit in Map" tool of UCSF Chimera, and this software was also used to generate all figures displaying the EM density[56].

Supplementary Material

Refer to Web version on PubMed Central for supplementary material.

ACKNOWLEDGEMENTS

We thank the members of the Martin lab for helpful discussions, C. Padovani for purified ubiquitin dimers, and R. Beckwith for proteasome base subcomplexes. We are also grateful to T. Wandless (Stanford School of Medicine) for providing the lysineless GFP construct, K. Nyquist for cloning the GFP model substrate used in degradation assays, and the Morgan lab (UCSF) for ubiquitin reagents. C.B. acknowledges support from the US National Science Foundation Graduate Research Fellowship, and M.E.M. acknowledges support from the American Cancer Society (grant 121453-PF-11-178-01-TBE). This research was also funded in part by the Damon Runyon Cancer Research Foundation (DFS-#07-13), the Pew Scholars program, the Searle Scholars program, and the US National Institutes of Health (grant DP2 EB020402-01) to G.C.L. A.M. acknowledges support from the Searle Scholars Program, start-up funds from the University of California Berkeley Molecular & Cell Biology Department, the US National Institutes of Health (grant R01-GM094497), the US National Science Foundation CAREER Program (NSF-MCB- 1150288).

REFERENCES

1. Finley D. Recognition and Processing of Ubiquitin-Protein Conjugates by the Proteasome. Annu. Rev. Biochem. 2009; 78:477–513. [PubMed: 19489727]
2. Goldberg AL. Protein degradation and protection against misfolded or damaged proteins. Nature. 2003; 426:895–899. [PubMed: 14685250]
3. Goldberg AL. Functions of the proteasome: from protein degradation and immune surveillance to cancer therapy. Biochem. Soc. Trans. 2007; 35:12–17. [PubMed: 17212580]
4. Verma R, et al. Role of Rpn11 metalloprotease in deubiquitination and degradation by the 26S proteasome. Science. 2002; 298:611–615. [PubMed: 12183636]
5. Yao T, Cohen RE. A cryptic protease couples deubiquitination and degradation by the proteasome. Nature. 2002; 419:403–407. [PubMed: 12353037]
6. Groll M, et al. Structure of 20S proteasome from yeast at 2.4Å resolution. Nature. 1997; 386:463–471. [PubMed: 9087403]
7. Martin A, Baker TA, Sauer RT. Pore loops of the AAA+ ClpX machine grip substrates to drive translocation and unfolding. Nat. Struct. Mol. Biol. 2008; 15:1147–1151. [PubMed: 18931677]
8. Maillard RA, et al. ClpX(P) generates mechanical force to unfold and translocate its protein substrates. Cell. 2011; 145:459–469. [PubMed: 21529717]
9. Aubin-Tam M-E, Olivares AO, Sauer RT, Baker TA, Lang MJ. Single-molecule protein unfolding and translocation by an ATP-fueled proteolytic machine. Cell. 2011; 145:257–267. [PubMed: 21496645]
10. Xu P, et al. Quantitative proteomics reveals the function of unconventional ubiquitin chains in proteasomal degradation. Cell. 2009; 137:133–145. [PubMed: 19345192]
11. Kim W, et al. Systematic and quantitative assessment of the ubiquitin-modified proteome. Mol. Cell. 2011; 44:325–340. [PubMed: 21906983]
12. Saeki Y, et al. Lysine 63-linked polyubiquitin chain may serve as a targeting signal for the 26S proteasome. EMBO J. 2009; 28:359–371. [PubMed: 19153599]
13. Zhang N, et al. Structure of the s5a:k48-linked diubiquitin complex and its interactions with rpn13. Mol. Cell. 2009; 35:280–290. [PubMed: 19683493]
14. Riedinger C, et al. Structure of Rpn10 and its interactions with polyubiquitin chains and the proteasome subunit Rpn12. J. Biol. Chem. 2010; 285:33992–34003. [PubMed: 20739285]
15. Elsasser S, Chandler-Militello D, Müller B, Hanna J, Finley D. Rad23 and Rpn10 serve as alternative ubiquitin receptors for the proteasome. J. Biol. Chem. 2004; 279:26817–26822. [PubMed: 15117949]
16. Zhang D, et al. Together, Rpn10 and Dsk2 can serve as a polyubiquitin chain-length sensor. Mol. Cell. 2009; 36:1018–1033. [PubMed: 20064467]
17. Mayor T, Graumann J, Bryan J, MacCoss MJ, Deshaies RJ. Quantitative profiling of ubiquitylated proteins reveals proteasome substrates and the substrate repertoire influenced by the Rpn10 receptor pathway. Mol. Cell. Proteomics. 2007; 6:1885–1895. [PubMed: 17644757]
18. Lander GC, et al. Complete subunit architecture of the proteasome regulatory particle. Nature. 2012; 482:186–191. [PubMed: 22237024]

19. Beck F, et al. Near-atomic resolution structural model of the yeast 26S proteasome. Proc. Natl. Acad. Sci. USA. 2012; 109:14870–14875. [PubMed: 22927375]
20. Beckwith R, Estrin E, Worden EJ, Martin A. Reconstitution of the 26S proteasome reveals functional asymmetries in its AAA+ unfoldase. Nat. Struct. Mol. Biol. 2013; 20:1164–1172. [PubMed: 24013205]
21. Matyskiela ME, Lander GC, Martin A. Conformational switching of the 26S proteasome enables substrate degradation. Nat. Struct. Mol. Biol. 2013; 20:781–788. [PubMed: 23770819]
22. Sledz P, Unverdorben P. Structure of the 26S proteasome with ATP-γS bound provides insights into the mechanism of nucleotide-dependent substrate translocation. Proc. Natl. Acad. Sci. USA. 2013; 110:7264–7269. [PubMed: 23589842]
23. Hu M, et al. Structure and mechanisms of the proteasome-associated deubiquitinating enzyme USP14. EMBO J. 2005; 24:3747–3756. [PubMed: 16211010]
24. Leggett DS, et al. Multiple associated proteins regulate proteasome structure and function. Mol. Cell. 2002; 10:495–507. [PubMed: 12408819]
25. Elsasser S, et al. Proteasome subunit Rpn1 binds ubiquitin-like protein domains. Nat. Cell Biol. 2002; 4:725–730. [PubMed: 12198498]
26. Hanna J, et al. Deubiquitinating enzyme Ubp6 functions noncatalytically to delay proteasomal degradation. Cell. 2006; 127:99–111. [PubMed: 17018280]
27. Peth A, Besche HC, Goldberg AL. Ubiquitinated proteins activate the proteasome by binding to Usp14/Ubp6, which causes 20S gate opening. Mol. Cell. 2009; 36:794–804. [PubMed: 20005843]
28. Peth A, Kukushkin N, Bossé M, Goldberg AL. Ubiquitinated proteins activate the proteasomal ATPases by binding to Usp14 or Uch37 homologs. J. Biol. Chem. 2013; 288:7781–7790. [PubMed: 23341450]
29. Lee B-H, et al. Enhancement of proteasome activity by a small-molecule inhibitor of USP14. Nature. 2010; 467:179–184. [PubMed: 20829789]
30. Torres EM, et al. Identification of aneuploidy-tolerating mutations. Cell. 2010; 143:71–83. [PubMed: 20850176]
31. Dephoure N, et al. Quantitative proteomic analysis reveals posttranslational responses to aneuploidy in yeast. eLife. 2014:e03023. [PubMed: 25073701]
32. Walters BJ, et al. A catalytic independent function of the deubiquitinating enzyme USP14 regulates hippocampal synaptic short-term plasticity and vesicle number. J. Physiol. 2014; 592:571–586. [PubMed: 24218545]
33. Levchenko I. A Specificity-Enhancing Factor for the ClpXP Degradation Machine. Science. 2000; 289:2354–2356. [PubMed: 11009422]
34. Dong KC, et al. Preparation of distinct ubiquitin chain reagents of high purity and yield. Structure. 2011; 19:1053–1063. [PubMed: 21827942]
35. Borodovsky A, et al. A novel active site-directed probe specific for deubiquitylating enzymes reveals proteasome association of USP14. EMBO J. 2001; 20:5187–5196. [PubMed: 11566882]
36. Asano S, et al. A molecular census of 26S proteasomes in intact neurons. Science. 2015; 347:439–443. [PubMed: 25613890]
37. Chu BW, et al. The E3 ubiquitin ligase UBE3C enhances proteasome processivity by ubiquitinating partially proteolyzed substrates. J. Biol. Chem. 2013; 288:34575–34587. [PubMed: 24158444]
38. Aufderheide A, et al. Structural characterization of the interaction of Ubp6 with the 26S proteasome. Proc. Natl. Acad. Sci. USA. 2015 201510449.
39. Marshall AG, et al. Genetic background alters the severity and onset of neuromuscular disease caused by the loss of ubiquitin-specific protease 14 (Usp14). PLOS ONE. 2013; 8:1–18.
40. Chen P-C, et al. The proteasome-associated deubiquitinating enzyme Usp14 is essential for the maintenance of synaptic ubiquitin levels and the development of neuromuscular junctions. J. Neurosci. 2009; 29:10909–10919. [PubMed: 19726649]
41. Crosas B, et al. Ubiquitin chains are remodeled at the proteasome by opposing ubiquitin ligase and deubiquitinating activities. Cell. 2006; 127:1401–1413. [PubMed: 17190603]

42. Aviram S, Kornitzer D. The ubiquitin ligase Hul5 promotes proteasomal processivity. Mol. Cell. Biol. 2010; 30:985–994. [PubMed: 20008553]
43. Inobe T, Fishbain S, Prakash S, Matouschek A. Defining the geometry of the two-component proteasome degron. Nat. Chem. Biol. 2011
44. Gomez TA, Kolawa N, Gee M, Sweredoski MJ, Deshaies RJ. Identification of a functional docking site in the Rpn1 LRR domain for the UBA-UBL domain protein Ddi1. BMC Biol. 2011; 9:33. [PubMed: 21627799]
45. Unverdorben P, et al. Deep classification of a large cryo-EM dataset defines the conformational landscape of the 26S proteasome. Proc. Natl. Acad. Sci. USA. 2014; 111:5544–5549. [PubMed: 24706844]
46. Worden EJ, Padovani C, Martin A. Structure of the Rpn11-Rpn8 dimer reveals mechanisms of substrate deubiquitination during proteasomal degradation. Nat. Struct. Mol. Biol. 2014; 21:220–227. [PubMed: 24463465]
47. Lander GC, et al. Appion: an integrated, database-driven pipeline to facilitate EM image processing. J. Struct. Biol. 2009; 166:95–102. [PubMed: 19263523]
48. Saeki, Y.; Isono, E.; Tohé, A. Ubiquitin and Protein Degradation, Part B. Vol. 399. Elsevier; 2005. p. 215p. 227
49. Verma R, et al. Proteasomal Proteomics: Identification of Nucleotide-sensitive Proteasome-interacting Proteins by Mass Spectrometric Analysis of Affinity-purified Proteasomes. Mol. Biol. Cell. 2000; 11:3425–3439. [PubMed: 11029046]
50. Kather I, Bippes CA, Schmid FX. A stable disulfide-free gene-3-protein of phage fd generated by in vitro evolution. J. Mol. Biol. 2005; 354:666–678. [PubMed: 16259997]
51. Worden EJ, Padovani C, Martin A. Structure of the Rpn11-Rpn8 dimer reveals mechanisms of substrate deubiquitination during proteasomal degradation. Nat. Struct. Mol. Biol. 2014; 21:220–227. [PubMed: 24463465]
52. Pickart CM, Raasi S. Controlled synthesis of polyubiquitin chains. Met. Enz. 2005; 399:21–36.
53. Carragher B, et al. Leginon: an automated system for acquisition of images from vitreous ice specimens. J. Struct. Biol. 2000; 132:33–45. [PubMed: 11121305]
54. Roseman AM. FindEM--a fast, efficient program for automatic selection of particles from electron micrographs. J. Struct. Biol. 2004; 145:91–99. [PubMed: 15065677]
55. Scheres SHW. RELION: implementation of a Bayesian approach to cryo-EM structure determination. J. Struct. Biol. 2012; 180:519–530. [PubMed: 23000701]
56. Goddard TD, Huang CC, Ferrin TE. Visualizing density maps with UCSF Chimera. J. Struct. Biol. 2007; 157:281–287. [PubMed: 16963278]

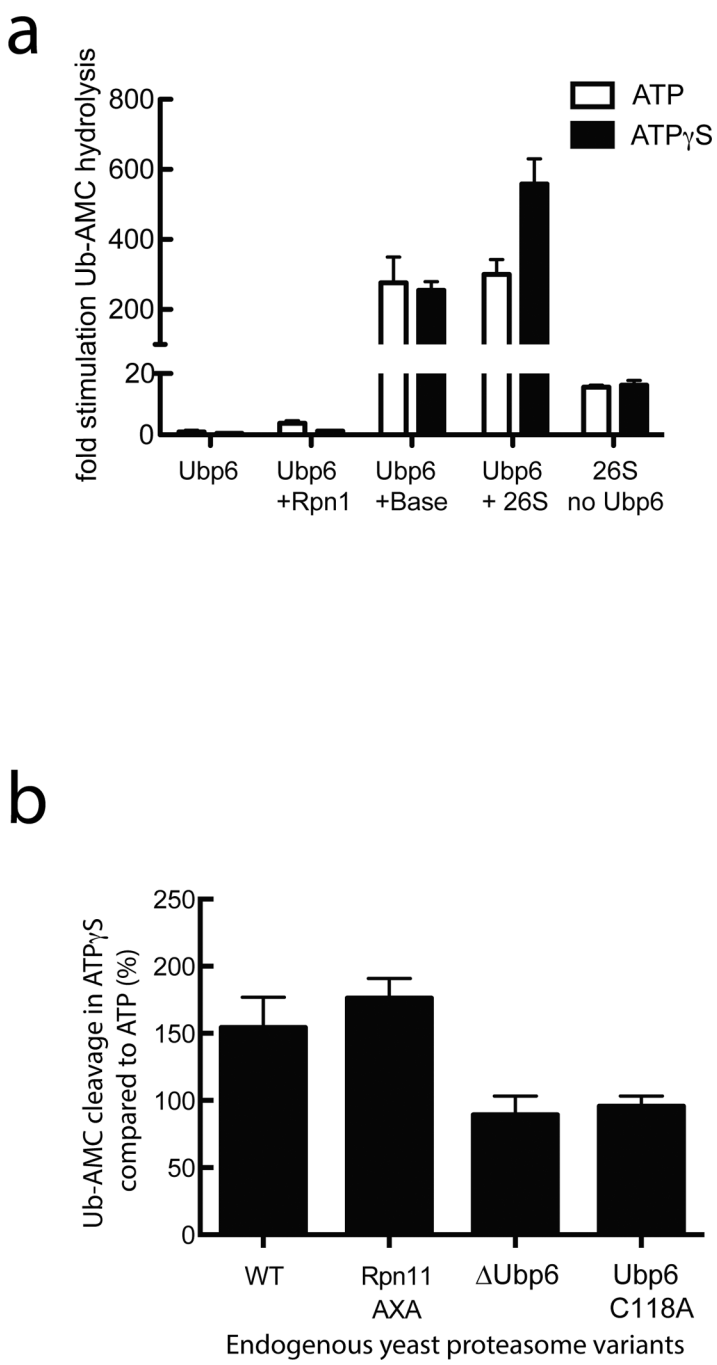

Figure 1. Ubp6 deubiquitination activity responds to the conformational state of the proteasome

Ub-AMC cleavage activity of Ubp6 was measured in response to interactions with the proteasomes holoenzyme or isolated subcomplexes. (a) Deubiquitination assays using proteasomes reconstituted with heterologously expressed base subcomplex purified from *E. coli* as well as core and lid subcomplexes purified from yeast, in the presence of ATP or the non-hydrolyzable ATPγS that induces the engaged state of the proteasome. (b) Deubiquitination assays using proteasomes purified from yeast strains with either wild-type, deleted, or inactive (C118A) Ubp6, or with wild-type Ubp6 and an inactive Rpn11 (AXA).

Shown are the relative activities in the presence of ATPγS compared to ATP. Data in a and b are means and s.e.m.of three independent experiments.

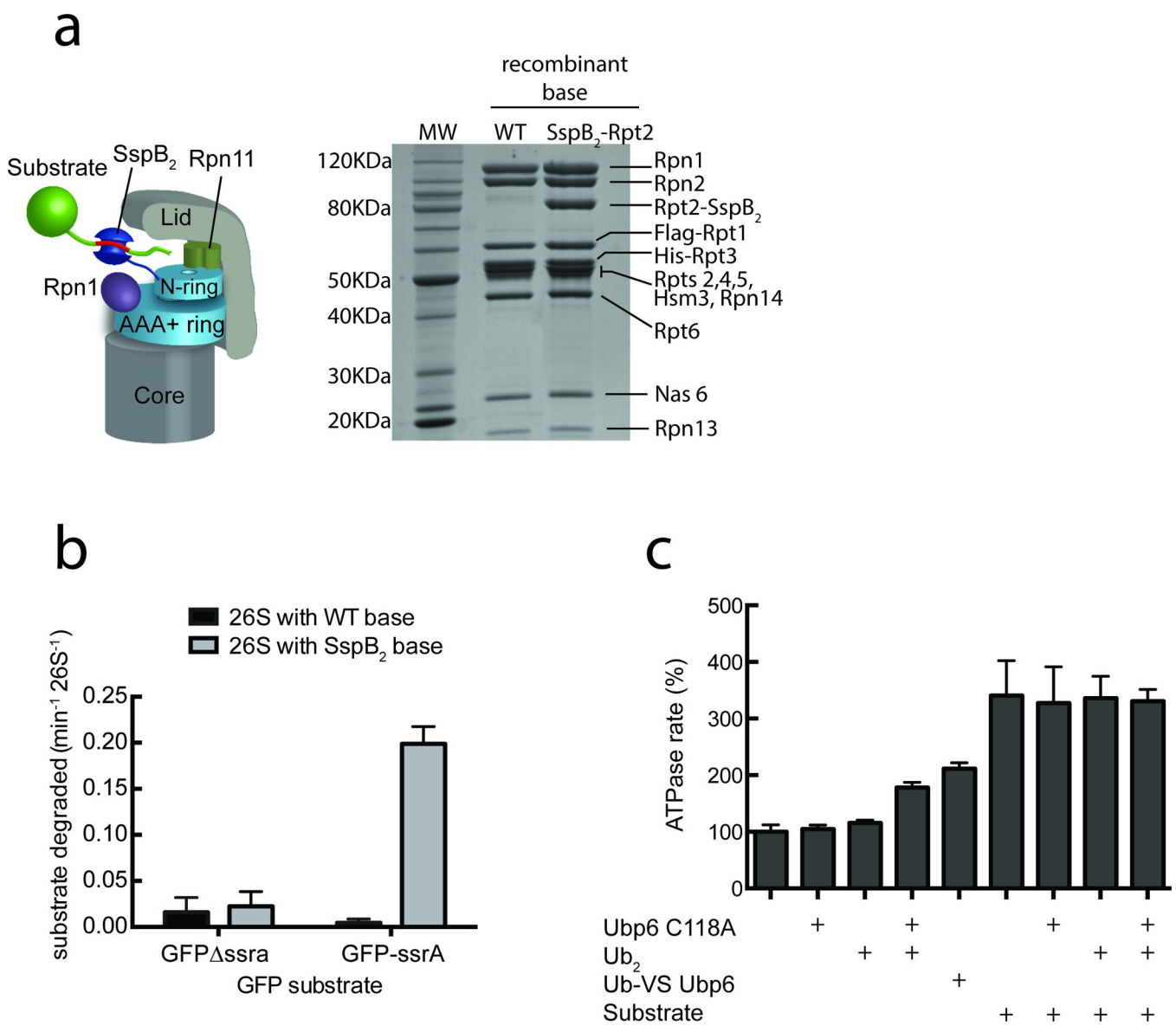

Figure 2. Ubp6 allostery is connected to substrate engagement

To separate ubiquitin processing from substrate engagement and translocation, we designed an ubiquitin-independent recruitment system by fusing a linked permutant of the bacterial dimeric substrate adapter $SspB_2$ to Rpt2 of the base. (a) Schematic of a $SspB_2$-fused proteasome recruiting an ssrA tagged substrate and SDS-PAGE of *E. coli*-expressed base subcomplex with either wild-type or $SspB_2$-fused Rpt2. (b) Degradation of a GFP model substrate containing the ssrA recognition motif was measured using proteasomes reconstituted with either wild-type or $SspB_2$-fused base complexes. (c) Ubiquitin-bound Ubp6 (Ubp6 C118A with di-ubiquitin or ubiquitin-vinylsulfone-fused Ubp6, Ubp6-UbVS) and substrate translocation stimulate the ATPase rate of $SspB_2$-fused proteasomes. Data shown in b and c are means and s.e.m. of three technical replicates.

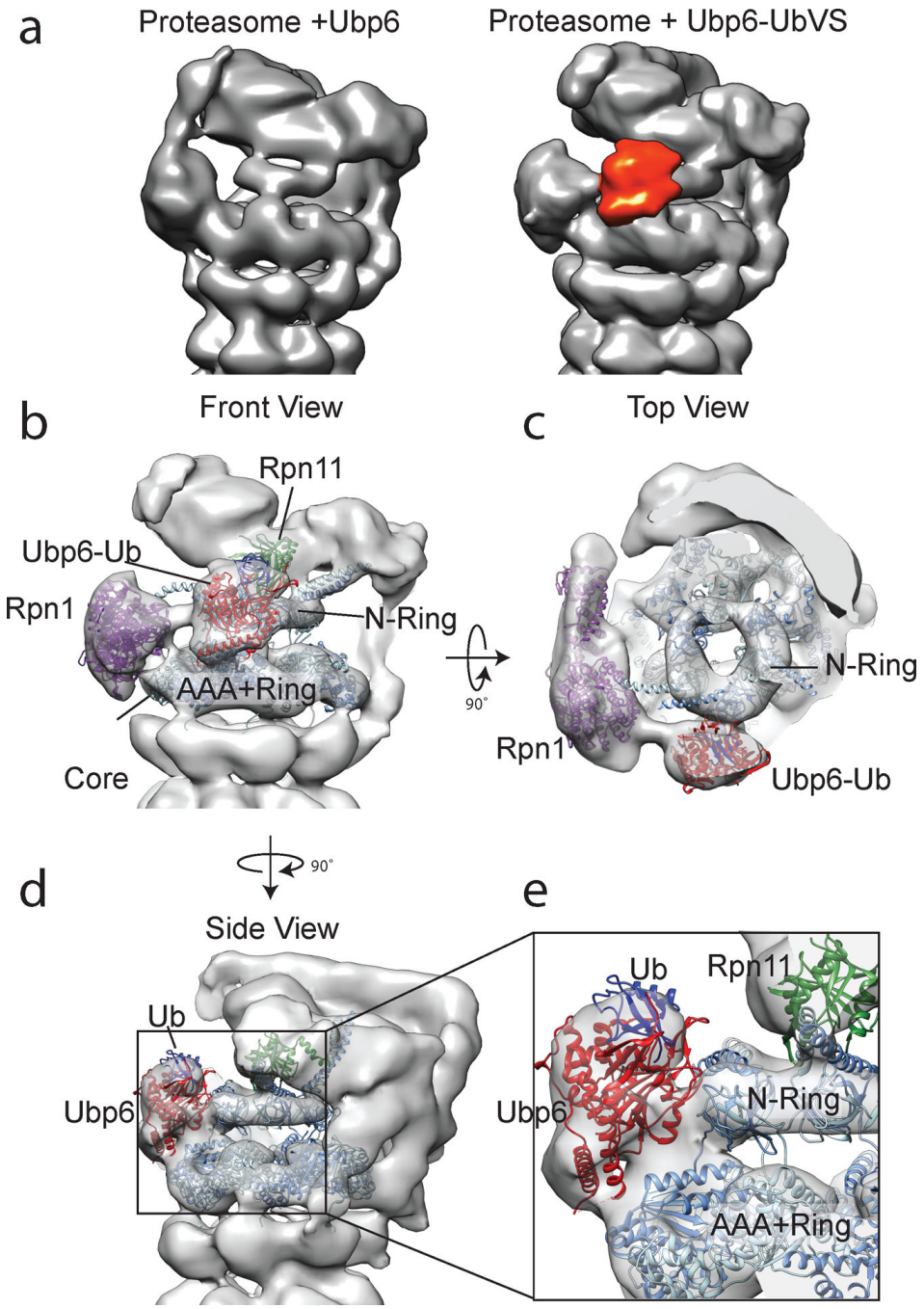

Figure 3. Ubiquitin-bound Ubp6 interacts with the Rpt hexamer of the base

(a) 3D reconstructions of the proteasome holoenzyme in complex with ATPγS and ubiquitin-free (left) or permanently ubiquitin-bound Ubp6 shown in red (right). (b–e) PDB models of various RP subunits were docked into the 3D electron density map obtained from negatively stained samples. Rpn1 is shown in purple (PDB 4CR4 Chain Z)[45], Rpn11 in green (PDB 4O8X)[46], and the ATPase ring in blue (PDB 4CR4, Chains H-M). The Ubp6-Ub homology model was docked into the corresponding density of the 22.3-Å resolution map (Ubp6 is shown in red, ubiquitin in blue). PDB models for all Rpt proteins of the base

are alternately colored in two different shades of blue. (b) Front view of the RP. Connecting density is observed between Rpn1 and the catalytic domain of Ubp6, which contacts the Rpt ring directly in front of Rpn11. (c) Top view of the RP. Ubp6 makes specific contacts with the N-terminal domain of Rpt1. (d) Side view of the RP. Ubp6 bridges the N-ring and the AAA+ ring in their coaxially stacked, engaged conformation. The N-domain residues of Rpt1 appear to interact with surface loops of Ubp6, while the AAA+ domain of Rpt1 contacts two C-terminal helices of Ubp6. This architecture places Ubp6 in close proximity to Rpn11 (~20 Å), with its bound ubiquitin only ~30 Å from the Rpn11 active site. (e) Zoomed-in view of (d), highlighting the Ubp6-base interface and proximity to Rpn11.

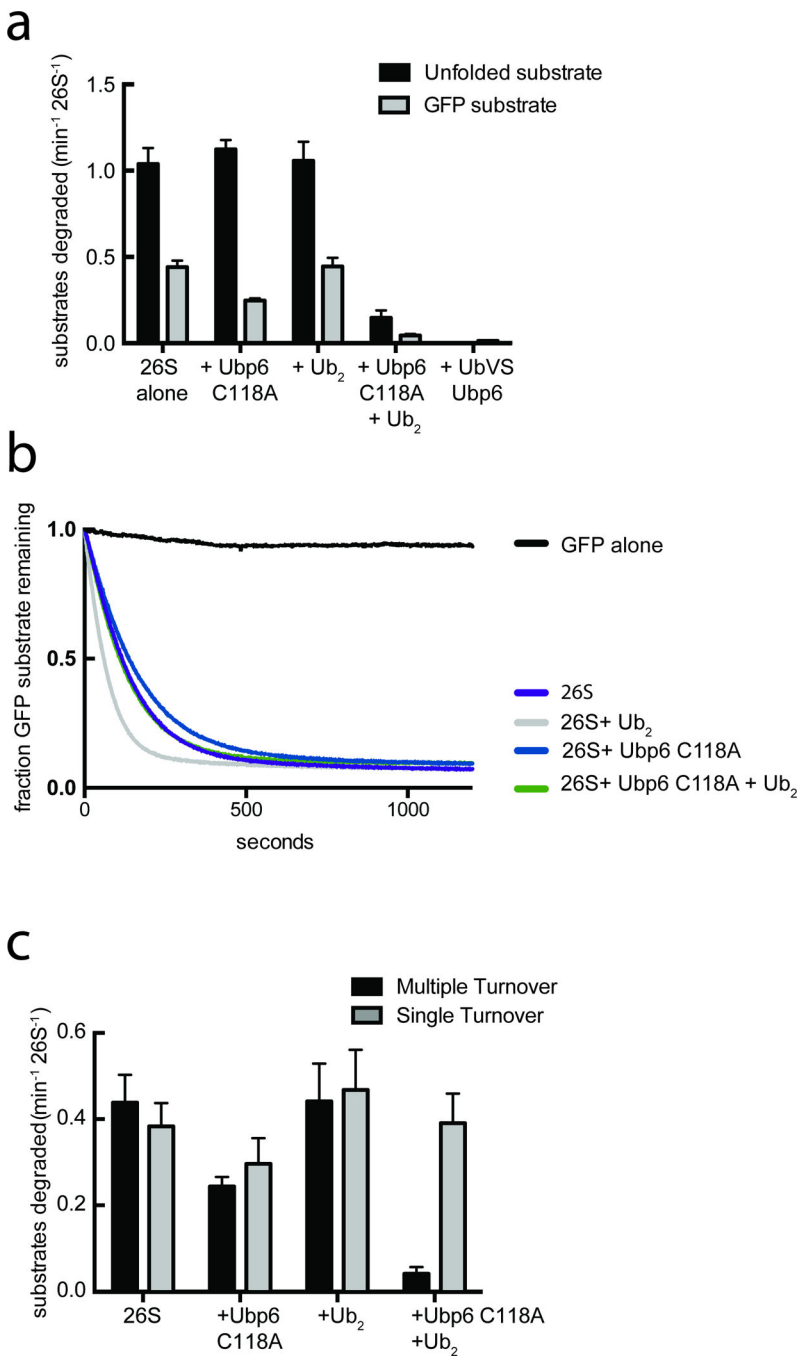

Figure 4. Ubiquitin-bound Ubp6 stabilizes the substrate-engaged conformation of the proteasome

Ubiquitin-independent substrate delivery to the proteasome reveals that ubiquitin-bound Ubp6 allosterically inhibits multiple- but not single-turnover degradation. (a) Multiple-turnover degradation of a permanently unfolded model substrate and a GFP fusion substrate by reconstituted $SspB_2$-Rpt2 proteasomes in the absence or presence of Ubp6 C118A and di-ubiquitin (Ub_2). Data shown are means and s.e.m of three technical replicates. Representative gels are shown in Supplementary Data Set 1. (b) Single-turnover degradation of the GFP fusion substrate by saturating amounts of reconstituted $SspB_2$-Rpt2 proteasomes

in the absence or presence of Ubp6 C118A and Ub_2. Curves shown are representative of three individual experiments. (c) Rate constants for degradation of the GFP fusion substrate under multiple- and single-turnover conditions shown in (a) and (b). Rate constants for single turnover degradations were determined from a single exponential regression of data; error bars represent s.e.m. of three individual experiments.

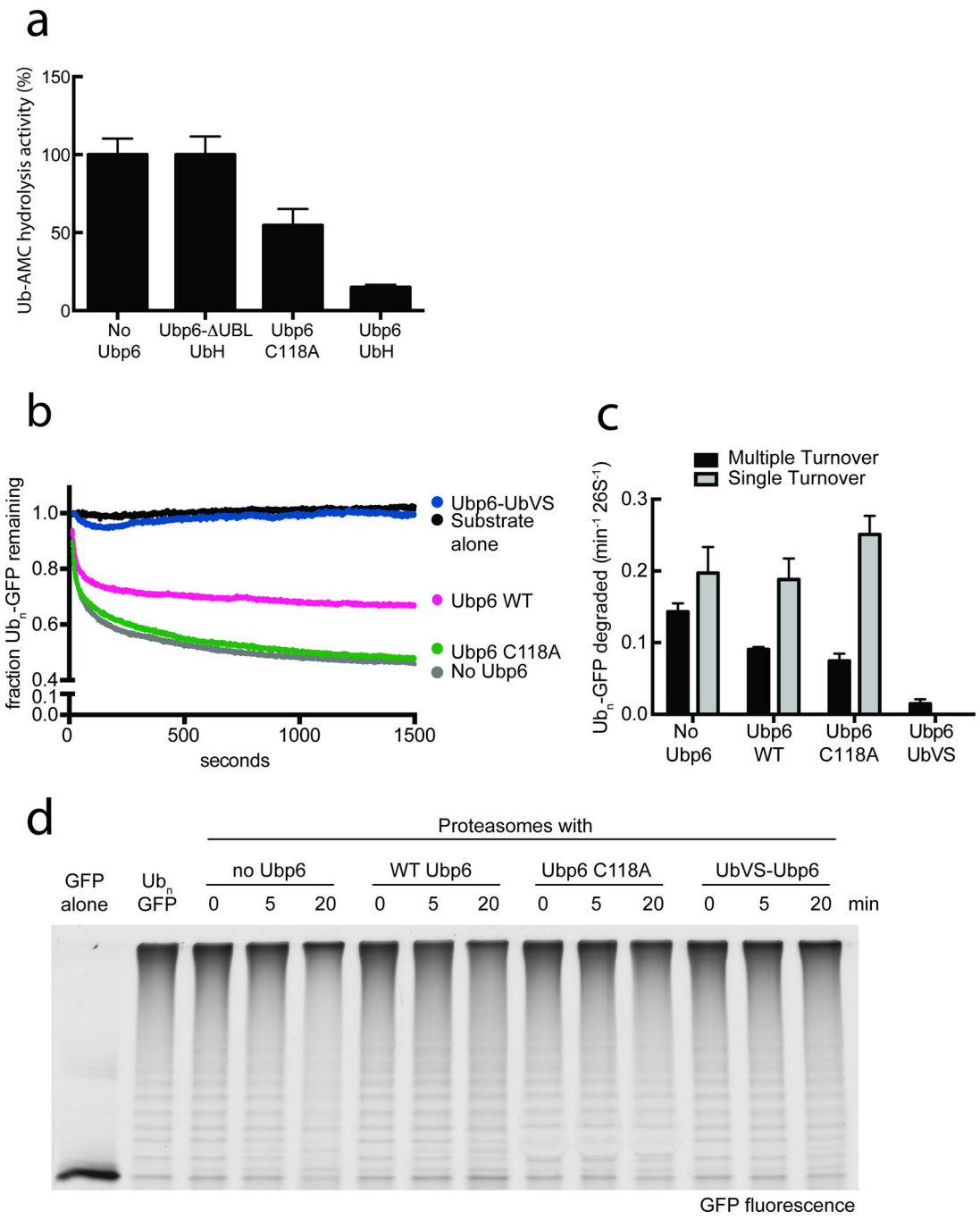

Figure 5. Ubp6 affects ubiquitin-dependent degradation

(a) Ubiquitin binding to Ubp6 strongly inhibits Rpn11 deubiquitination activity. Ubp6 (wild type or C118A) was treated with ubiquitin aldehyde (Ub-H) and added to Ubp6-free holoenzymes purified from yeast. Rpn11 deubiquitination activity was measured by Ub-AMC cleavage. Data are means and s.e.m. of 3 independent experiments. (b,c) The same GFP fusion substrate used for ubiquitin-independent turnover in figure 4 was ubiquitinated *in vitro* at an engineered single lysine residue, to examine the effects of Ubp6 on ubiquitin-dependent substrate degradation. (b) Single-turnover degradation of the polyubiquitinated

GFP fusion substrate were measured with saturating amounts of proteasome holoenzyme purified from an Ubp6-knockout yeast strain, with no Ubp6, wild-type Ubp6, Ubp6 C118A, or Ubp6-UbVS added back. (c) Rate constants for single- and multiple-turnover degradation of the ubiquitinated GFP model substrate. Data shown are means and s.e.m. from three technical replicates. (d) Degradation of a poly-ubiquitinated EGFP^{20,47} substrate was assessed by SDS-PAGE and in-gel GFP fluorescence detection. Used proteasomes were purified from ubp6Δ yeast cells and incubated with either buffer, WT, C118A or UbVS-treated Ubp6.

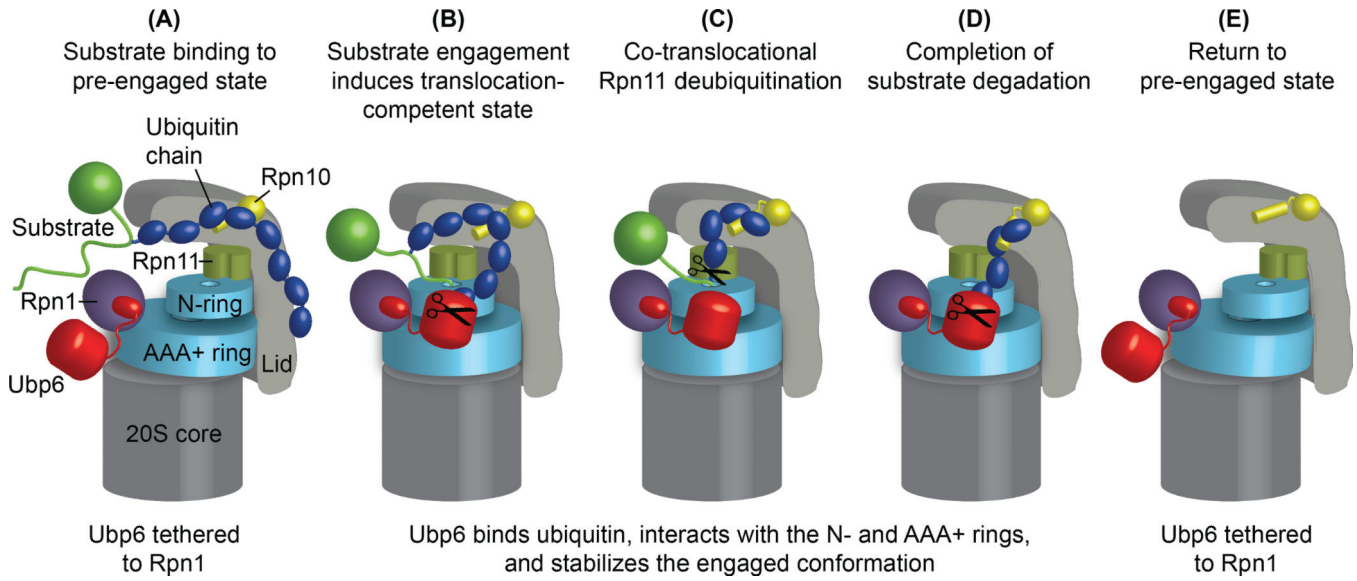

Figure 6. Model for Ubp6 acting as an ubiquitin-dependent timer to allosterically control proteasome conformational changes, Rpn11 deubiquitination, and substrate degradation

(a) Ubiquitin-chain binding to an intrinsic receptor (e.g. Rpn10) tethers a substrate to the proteasome. Ubp6 is bound to the proteasome via its Ubl domain interacting with Rpn1. (b) Engagement of the unstructured initiation region of the substrate by the ATPase hexamer induces a conformational switch of the regulatory particle to a substrate-engaged, translocation competent state, characterized by a coaxial alignment of Rpn11, N-ring, AAA + ring and 20S core. If ubiquitin-bound, for instance during debranching or trimming of ubiquitin chains, Ubp6 interacts with and stabilizes the engaged state of the ATPase hexamer by bridging the N-ring and AAA+ ring. In this state, ubiquitin-bound Ubp6 inhibits Rpn11-mediated deubiquitination and consequently substrate degradation. (c) Translocation moves the ubiquitin-modified lysines of the substrate into the Rpn11 active site for co-translocational ubiquitin-chain removal. (d) Even after complete substrate translocation, ubiquitin-bound Ubp6 stabilizes the engaged conformation of the proteasome, prevents switching back to the engagement-competent state, and thus interferes with the degradation of the subsequent substrate. Such trapping of the engaged state would allow Ubp6 to clear ubiquitin chains from proteasomal receptors before the next substrate is engaged and degradation is initiated. (e) As soon as it is no longer occupied with ubiquitin, the catalytic domain of Ubp6 releases from the N-ring and AAA+ ring, and allows the regulatory particle to return to the pre-engaged state for the next round of substrate degradation.